Optical Phonon Lasing in Semiconductor Double Quantum Dots

Rin Okuyama,[1,*] Mikio Eto,[1] and Tobias Brandes[2]

[1] *Faculty of Science and Technology, Keio University, Yokohama 223-8522, Japan*
[2] *Institut für Theoretische Physik, Technische Universität Berlin, D-10623 Berlin, Germany*

(Dated: December 21, 2012)

We propose optical phonon lasing for a double quantum dot (DQD) fabricated in a semiconductor substrate. We show that the DQD is weakly coupled to only two LO phonon modes that act as a natural cavity. The lasing occurs for pumping the DQD via electronic tunneling at rates much higher than the phonon decay rate, whereas an antibunching of phonon emission is observed in the opposite regime of slow tunneling. Both effects disappear with an effective thermalization induced by the Franck-Condon effect in a DQD fabricated in a carbon nanotube with a strong electron-phonon coupling.

Keywords: quantum dot, optical phonon, cavity quantum electrodynamics, microlaser, Franck-Condon effect, phonon-assisted transport, polaron

Electrically tunable two-level systems are ideal candidates to study the interaction between fermions and bosons under nonequilibrium conditions. Single-qubit lasers or nanomechanical resonators [1–7] are examples where concepts from quantum optics, such as the microlaser [8], have been successfully transferred to and combined with artificial solid-state architectures. Semiconductor double quantum dots (DQDs) play a similar role as model systems with the coupling between electrons and the surrounding substrate leading to, e.g., tunable spontaneous phonon emission and Dicke-type interference effects [9–11].

In this Letter, we propose optical phonon lasing in a DQD without the requirement of an additional cavity or resonator. We start from the observation that a DQD effectively couples to only two LO phonon modes that work as a natural cavity. The pumping to the upper level is realized by an electric current through the DQD under a finite bias. The amplified LO phonons occasionally escape from this cavity by decaying into the so-called "daughter phonons" [12] that can be observed externally. The phonon lasing is possible when the pumping rate is much higher than the phonon decay rate $\Gamma_{\rm ph}$.

We also observe the phonon antibunching in the same system when the pumping rate is lower than $\Gamma_{\rm ph}$. We emphasize that the phonon statistics can be changed by electrically tuning the tunnel coupling between DQDs and leads [13]. Note that LO-phonon-assisted transport through a DQD was theoretically studied by Gnodtke *et al.* [14] and has recently been observed by Amaha and Ono [15]. We also note that phonon lasing by optical pumping was suggested in single quantum dots [16].

Both the phonon lasing and antibunching are weak coupling effects that are spoilt by phonon thermalization via the Franck-Condon effect [17–19] for a strong electron-phonon coupling. In electric transport, the number of electrons in the DQD fluctuates, which is accompanied by lattice distortions and thus the creation of bunched phonons. We show that this effect is negligible in DQDs fabricated on GaAs substrates (weak coupling case) but surpasses the lasing and antibunching in DQDs on carbon nanotubes (CNTs; strong coupling case) [20].

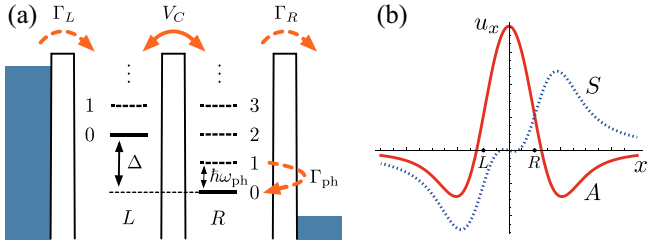

FIG. 1. (Color online). (a) Model for a double quantum dot (DQD) coupled to LO phonons. A large bias is applied between external leads. The spacing Δ between the energy levels in dots L and R is electrically tunable. When Δ matches an integer (ν) multiple of the phonon energy $\hbar\omega_{\rm ph}$, the electronic state $|L\rangle$ with n phonons is coherently coupled to $|R\rangle$ with $(n+\nu)$ phonons. (b) Phonon mode functions $\boldsymbol{u}(\boldsymbol{r})$ along a line through the centers of quantum dots located at $x=\pm\mathcal{R}$, when the wavefunctions $|L\rangle$ and $|R\rangle$ are spherical with radius $\mathcal{R}$. The x-component of $\boldsymbol{u}(x,0,0)$ is shown for $S(A)$-phonons that couple (anti-)symmetrically to the DQD. Note that u_x is an odd (even) function of x for $S(A)$-phonons since the induced charge is proportional to $\boldsymbol{\nabla}\cdot\boldsymbol{u}$.

Figure 1(a) depicts our model of a DQD embedded in a substrate, in which two single-level quantum dots, L and R, are connected by tunnel coupling V_C. The level spacing Δ between the dots is assumed to be tunable, and the total number of electrons in the DQD is restricted to one or zero by the Coulomb blockade. The electron couples to LO phonons of energy $\hbar\omega_{\rm ph}$ in the substrate via the Fröhlich interaction. Our system Hamiltonian is

$\mathcal{H} = \mathcal{H}_e + \mathcal{H}_{\rm ph} + \mathcal{H}_{\rm ep}$,

$$\mathcal{H}_e = \frac{\Delta}{2}(n_L - n_R) + V_C(d_L^\dagger d_R + d_R^\dagger d_L), \quad (1)$$

$$\mathcal{H}_{\rm ph} = \hbar\omega_{\rm ph}\sum_{\boldsymbol{q}} N_{\boldsymbol{q}}, \quad (2)$$

$$\mathcal{H}_{\rm ep} = \sum_{\alpha=L,R}\sum_{\boldsymbol{q}} M_{\alpha,\boldsymbol{q}}(a_{\boldsymbol{q}} + a_{-\boldsymbol{q}}^\dagger)n_\alpha, \quad (3)$$

using creation (annihilation) operators $d_\alpha^\dagger$ (d_α) for an electron in dot α and $a_{\boldsymbol{q}}^\dagger$ ($a_{\boldsymbol{q}}$) for a phonon with wave vector $\boldsymbol{q}$. $n_\alpha = d_\alpha^\dagger d_\alpha$ and $N_{\boldsymbol{q}} = a_{\boldsymbol{q}}^\dagger a_{\boldsymbol{q}}$ are the number operators. The spin index is omitted for electrons. The coupling constant is given by $M_{\alpha,\boldsymbol{q}} = \sqrt{\frac{e^2\hbar\omega_{\rm ph}}{2V}(\frac{1}{\epsilon(\infty)} - \frac{1}{\epsilon(0)})}\frac{1}{q}\langle\alpha|e^{i\boldsymbol{q}\cdot\boldsymbol{r}}|\alpha\rangle$, where $|\alpha\rangle$ is the electron wavefunction in dot α, $\epsilon(\infty)$ [$\epsilon(0)$] is the dielectric constant at a high [low] frequency, and V is the substrate volume. The LO phonons only around the Γ point ($|\boldsymbol{q}| \lesssim 1/\mathcal{R}$ with dot radius $\mathcal{R}$) are coupled to the DQD because of an oscillating factor in $M_{\alpha,\boldsymbol{q}}$. This fact justifies the dispersionless phonons in $\mathcal{H}_{\rm ph}$. We assume equivalent quantum dots L and R, whence $M_{R,\boldsymbol{q}} = M_{L,\boldsymbol{q}}e^{i\boldsymbol{q}\cdot\boldsymbol{r}_{LR}}$ with $\boldsymbol{r}_{LR}$ being a vector joining their centers.

In $\mathcal{H}_{\rm ep}$, an electron in dot α couples to a single mode of a phonon described by

$$a_\alpha = \frac{\sum_{\boldsymbol{q}} M_{\alpha,\boldsymbol{q}}a_{\boldsymbol{q}}}{(\sum_{\boldsymbol{q}}|M_{\alpha,\boldsymbol{q}}|^2)^{1/2}}. \quad (4)$$

We perform a unitary transformation for phonons from $a_{\boldsymbol{q}}$ to collective phonon coordinates,

$$a_S = \frac{a_L + a_R}{\sqrt{2(1+\mathcal{S})}}, \quad a_A = \frac{a_L - a_R}{\sqrt{2(1-\mathcal{S})}}, \quad (5)$$

and other modes orthogonal to a_S and a_A, where $\mathcal{S}$ is the overlap integral between a_L and a_R phonons in Eq. (4). Disregarding the modes decoupled from the DQD, we obtain the effective Hamiltonian

$$H = \mathcal{H}_e + \hbar\omega_{\rm ph}\left[N_S + \lambda_S(a_S + a_S^\dagger)(n_L + n_R)\right] + \hbar\omega_{\rm ph}\left[N_A + \lambda_A(a_A + a_A^\dagger)(n_L - n_R)\right], \quad (6)$$

with $N_S = a_S^\dagger a_S$, $N_A = a_A^\dagger a_A$, and dimensionless coupling constants $\lambda_{S/A} = (\sum_{\boldsymbol{q}}|M_{L,\boldsymbol{q}} \pm M_{R,\boldsymbol{q}}|^2)^{1/2}/(2\hbar\omega_{\rm ph})$.

The mode functions for S- and A-phonons are depicted in Fig. 1(b) along a line through the centers of the quantum dots. Since the phonons are dispersionless, they do not diffuse and act as a cavity including the DQD [21]. A-phonons play a crucial role in phonon-assisted tunneling and phonon lasing, as discussed below, whereas S-phonons do not since they couple to the *total* number of electrons in the DQD, $n_L + n_R$. Both phonons are relevant to the Franck-Condon effect.

Our Hamiltonian H in Eq. (6) is applicable to DQDs fabricated on a semiconductor substrate, where $\hbar\omega_{\rm ph} =$ 36 meV and $\lambda_{S,A} = 0.1 - 0.01$ for $\mathcal{R} = 10 - 100$ nm in GaAs [22]. It also describes a DQD in a suspended CNT when an electron couples to a vibron, which is a longitudinal stretching mode with $\hbar\omega_{\rm ph} \sim 1$ meV, $\lambda_A \gtrsim 1$, and $\lambda_S = 0$ in experimental situations [18, 19].

The DQD is connected to external leads in series, which enables electronic pumping. Under a large bias, an electron tunnels into dot L from the left lead with tunneling rate Γ_L and tunnels out from dot R to the right lead with Γ_R [23]. We also introduce the phonon decay rate $\Gamma_{\rm ph}$ to take into account the natural decay of LO phonons due to lattice anharmonicity [12]. We describe the dynamics of the DQD-phonon density matrix ρ using the Markovian master equation

$$\dot\rho = -\frac{i}{\hbar}[H,\rho] + \mathcal{L}_e\rho + \mathcal{L}_{\rm ph}\rho, \quad (7)$$

where $\mathcal{L}_e\rho = (\Gamma_L\mathcal{D}[d_L^\dagger] + \Gamma_R\mathcal{D}[d_R])\rho$ and $\mathcal{L}_{\rm ph}\rho = \Gamma_{\rm ph}(\mathcal{D}[a_S] + \mathcal{D}[a_A])\rho$, with $\mathcal{D}[A]\rho = A\rho A^\dagger - \frac{1}{2}\{\rho, A^\dagger A\}$ being a Lindblad dissipator. Here, we assumed that the temperature of the substrate, k_BT, is much lower than $\hbar\omega_{\rm ph}$.

In the following, we apply the Born-Markov-Secular approximation to Eq. (7) by diagonalizing the Hamiltonian H and setting up the corresponding rate equation in the energy eigenbasis,

$$\dot P_i = \sum_j L_{ij}P_j, \quad (8)$$

for the probabilities P_i to find the system in an eigenstate $|i\rangle$, with $L_{ij} = \langle i|[(\mathcal{L}_e + \mathcal{L}_{\rm ph})|j\rangle\langle j|]|i\rangle$. The solution of Eq. (8) with $\dot P_i = 0$ determines the steady state properties.

First, we discuss our numerical results in the case of $\Gamma_{L,R} \gg \Gamma_{\rm ph}$. We consider A-phonons and disregard S-phonons ($\lambda_S = 0$). Figure 2(a) shows the current I through the DQD as a function of level spacing Δ, with $\lambda_A = 0.1$ and 1. Beside the main peak at $\Delta = 0$, we observe subpeaks at $\Delta \simeq \nu\hbar\omega_{\rm ph}$ ($\nu = 1, 2, 3, \ldots$) due to the phonon-assisted tunneling. At the νth subpeak, electron transport through the DQD is accompanied by the emission of ν phonons. As a result, the phonon number is markedly increased at the subpeaks, as shown in Fig. 2(b), in both cases of $\lambda_A = 0.1$ and 1. However, the physics is very different for the two cases, as we will show below.

For $\lambda_A = 0.1$ and $\Delta \simeq \nu\hbar\omega_{\rm ph}$, the electronic state $|L\rangle$ with n phonons is coherently coupled to $|R\rangle$ with $(n+\nu)$ phonons [24], similarly to a microlaser two-level system in a photon cavity, if the lattice distortion can be neglected. To examine the amplification of A-phonons, we calculate the phonon autocorrelation function

$$g_A^{(2)}(\tau) = \langle : N_A(0)N_A(\tau) : \rangle / \langle N_A\rangle^2, \quad (9)$$

which is the probability of phonon emission at time τ on the condition that a phonon is emitted at time 0 [25,

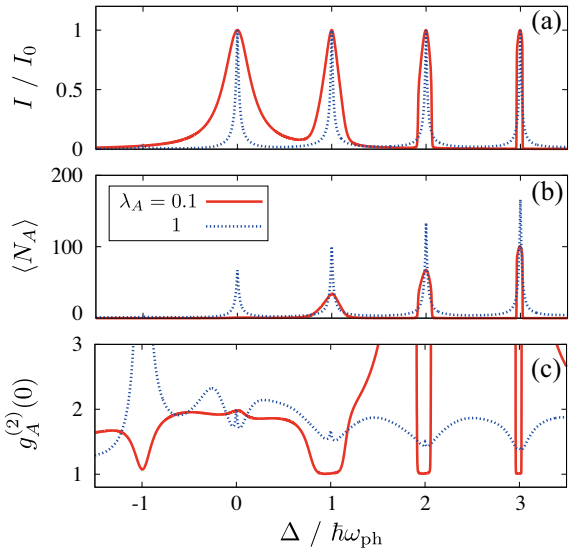

FIG. 2. (Color online). (a) Electric current through the DQD, (b) A-phonon number $\langle N_A\rangle$, and (c) its autocorrelation function $g_A^{(2)}(0)$ as a function of level spacing Δ in the DQD. The dimensionless electron-phonon couplings are $\lambda_A = 0.1$ (solid lines) or 1 (dotted lines), and $\lambda_S = 0$. $I_0 = e\Gamma_R/(2+\alpha)$ is the current at $\Delta = 0$ in the absence of electron-phonon coupling. $\Gamma_L = \Gamma_R = 100\ \Gamma_{\rm ph}$ and $V_C = 0.1\ \hbar\omega_{\rm ph}$.

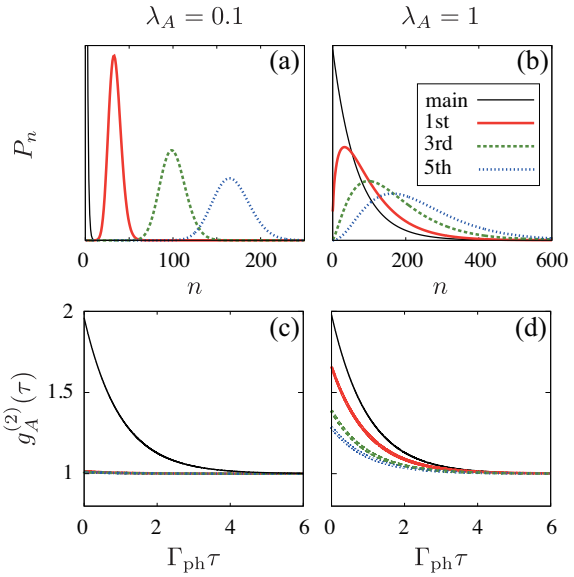

FIG. 3. (Color online). (a), (b) Number distribution of A-phonons and (c), (d) its autocorrelation function $g_A^{(2)}(\tau)$ at the current main peak and subpeaks ($\nu = 1, 3, 5$). The dimensionless electron-phonon couplings are $\lambda_A = 0.1$ [1] in panels (a) and (c) [(b) and (d)] and $\lambda_S = 0$. Note that three lines for the current subpeaks are almost overlapped in panel (c). $\Gamma_L = \Gamma_R = 100\ \Gamma_{\rm ph}$ and $V_C = 0.1\ \hbar\omega_{\rm ph}$.

26]. $g_A^{(2)}(0) = 1$ indicates a *Poissonian* distribution of phonons, which is a criterion of phonon lasing. We thus find phonon lasing at the current subpeaks in Fig. 2(c). We mention that these are not changed in the presence of finite coupling λ_S to S-phonons.

When $\lambda_A = 1$, the strength of the electron-phonon interaction is comparable to the phonon energy. In this case, the lattice distortion by the Franck-Condon effect severely disturbs the above-mentioned coherent coupling between an electron and phonons in the DQD and, as a result, suppresses the phonon lasing. Indeed, $g_A^{(2)}(0) > 1$ at the current subpeaks, indicating the phonon bunching.

To compare the two situations in detail, we show the number distribution of A-phonons in Figs. 3(a) and 3(b) at the current main peak and subpeaks. In the case of $\lambda_A = 0.1$, a Poisson-like distribution emerges at the subpeaks, whereas a Bose distribution with effective temperature T^* is seen at the main peak. T^* is determined from the number of phonons in the stationary state as $1/[e^{\hbar\omega_{\rm ph}/(k_B T^*)} - 1] = \langle N_A\rangle$. When $\lambda_A = 1$, on the other hand, the distribution shows an intermediate shape between Poissonian and Bose distributions at the subpeaks and a Bose distribution at the main peak. In Figs. 3(c) and 3(d), we plot the autocorrelation function $g_A^{(2)}(\tau)$ of A-phonons as a function of τ. In the case of $\lambda_A = 0.1$, $g_A^{(2)}(\tau) \simeq 1$, regardless of the time delay τ, supports the phonon lasing at the current subpeaks. At the main peak, $g_A^{(2)}(\tau) \simeq 1 + e^{-\Gamma_{\rm ph}\tau}$, which is a character of thermal phonons with effective temperature T^*. When $\lambda_A = 1$, we find an intermediate behavior, $g_A^{(2)}(\tau) \simeq 1 + \delta_\nu e^{-\Gamma_{\rm ph}\tau}$ ($0 < \delta_\nu < 1$), at the νth subpeak. This indicates that the phonons are partly thermalized by the Franck-Condon effect. For larger ν values, the distribution is closer to the Poissonian with smaller δ_ν.

To elucidate the competition between the phonon lasing and thermalization by the Franck-Condon effect, we analyze the rate equation in Eq. (8), focusing on the current peaks. We introduce polaron states $|L(R), n\rangle$ for an electron in dot L (R) and n phonons with lattice distortion:

$$|L(R), n\rangle = |L(R)\rangle \otimes \mathcal{T}^{(\dagger)}|n\rangle_A, \quad \mathcal{T} = e^{-\lambda_A(a_A^\dagger - a_A)}, \tag{10}$$

where $\mathcal{T}$ and $\mathcal{T}^\dagger$ describe the shift of the equilibrium position of the lattice when an electron stays in dots L and R, respectively. Note that the lattice distortion produces λ_A^2 extra phonons: $\langle\alpha, n|N_A|\alpha, n\rangle = n + \lambda_A^2$. When $\Delta \simeq \nu\hbar\omega_{\rm ph}$, the eigenstates of Hamiltonian H are given by the zero-electron states $|0, n\rangle = |0\rangle\otimes|n\rangle_A$ and bonding and antibonding states between the polarons

$$|\pm, n\rangle = \frac{1}{\sqrt{2}}(|L, n\rangle \pm |R, n+\nu\rangle) \tag{11}$$

($n = 0, 1, 2, \ldots$) and the polarons localized in dot R, $|R, n\rangle$ ($n = 0, 1, 2, \ldots, \nu - 1$), in a good approximation, provided that $V_C \ll \hbar\omega_{\rm ph}$. The rate equations for these

states are

$$\dot{P}_{0,n} = -\Gamma_L P_{0,n} + \sum_{m=0}^{\infty} \frac{\Gamma_R}{2} |{}_A\langle n|\mathcal{T}^\dagger|m+\nu\rangle_A|^2 P_{\mathrm{mol},m} + \sum_{m=0}^{\nu-1} \Gamma_R |{}_A\langle n|\mathcal{T}^\dagger|m\rangle_A|^2 P_{R,m} + \Gamma_{\mathrm{ph}}\left[(n+1)P_{0,n+1} - nP_{0,n}\right], \quad (12)$$

$$\dot{P}_{\mathrm{mol},n} = -\frac{\Gamma_R}{2} P_{\mathrm{mol},n} + \sum_{m=0}^{\infty} \Gamma_L |{}_A\langle n|\mathcal{T}|m\rangle_A|^2 P_{0,m} + \Gamma_{\mathrm{ph}}\left[\left(n+1+\frac{\nu}{2}\right) P_{\mathrm{mol},n+1} - \left(n+\frac{\nu}{2}\right) P_{\mathrm{mol},n}\right], \quad (13)$$

where $P_{\mathrm{mol},n} = P_{+,n} + P_{-,n}$ $(n = 0, 1, 2, \ldots)$ and

$$\dot{P}_{R,n} = -\Gamma_R P_{R,n} + \Gamma_{\mathrm{ph}}\big[(n+1)P_{R,n+1} - nP_{R,n}\big], \quad (14)$$

with $P_{R,\nu} = P_{\mathrm{mol},0}/2$ $(n = 0, 1, 2, \ldots, \nu-1)$. These equations yield the current I and the electron number in the DQD $\langle n_e\rangle = \langle n_L + n_R\rangle$ in terms of the number of polarons localized in dot R, $\langle \tilde{n}_R\rangle = \sum_{n=0}^{\nu-1} P_{R,n}$ as

$$I = e\Gamma_R \frac{1+\langle \tilde{n}_R\rangle}{2+\alpha}, \quad \langle n_e\rangle = \frac{2-\alpha\langle \tilde{n}_R\rangle}{2+\alpha} \quad (15)$$

with $\alpha = \Gamma_R/\Gamma_L$. The number of A-phonons is given by

$$\langle N_A\rangle = (\nu + 2\lambda_A^2)\frac{I}{e\Gamma_{\mathrm{ph}}} + \lambda_A^2\langle n_e\rangle. \quad (16)$$

The first two terms in Eq. (16) indicate the emission of ν phonons by the phonon-assisted tunneling (from dot L to dot R) and creation of $2\lambda_A^2$ phonons by lattice distortion (with two tunnelings between the DQD and leads) per transfer of a single electron through the DQD. The last term describes the average number of polarons $\langle n_e\rangle$ in the stationary state.

When $\Gamma_{L,R} \gg \Gamma_{\mathrm{ph}}$, we obtain $I = I_0 + \mathcal{O}(\Gamma_{\mathrm{ph}}/\Gamma_{L,R})$, where $I_0 = e\Gamma_R/(2+\alpha)$ is the current at the main peak in the absence of electron-phonon interaction, and [27]

$$g_A^{(2)}(0) = \frac{\nu + 4\lambda_A^2}{\nu + 2\lambda_A^2} + \mathcal{O}(\Gamma_{\mathrm{ph}}/\Gamma_{L,R}). \quad (17)$$

These explain the numerical results in Fig. 2 at the current subpeaks. Equation (17) indicates $g_A^{(2)}(0) \simeq 1$ (phonon lasing) for $\lambda_A^2 \ll \nu$ and $g_A^{(2)}(0) \simeq 2$ (phonons thermalized by lattice distortion) for $\lambda_A^2 \gg \nu$. In the latter case, the phonons follow the Bose distribution with T^* for the deduction of $\langle N_A\rangle$ in Eq. (16).

Thus far, we have discussed the phonon lasing in the case of $\Gamma_{L,R} \gg \Gamma_{\mathrm{ph}}$. If the tunnel coupling is tuned to be $\Gamma_{L,R} \lesssim \Gamma_{\mathrm{ph}}$, we observe another phenomenon, i.e., antibunching of LO phonons [28]. Figure 4(a) presents a color-scale plot of $g_A^{(2)}(0)$ at the first current subpeak

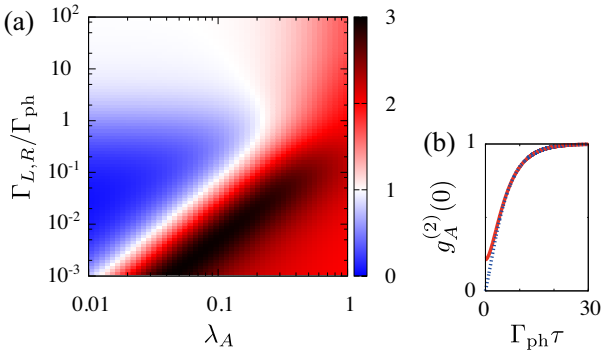

FIG. 4. (Color online). (a) Color-scale plot of autocorrelation function of A-phonons, $g_A^{(2)}(0)$, at the first subpeak of current in a plane of electron-phonon coupling λ_A and $\Gamma_{L,R}/\Gamma_{\mathrm{ph}}$. $\Gamma_L = \Gamma_R \equiv \Gamma_{L,R}$, $\lambda_S = 0$, and $V_C = 0.1\ \hbar\omega_{\mathrm{ph}}$. (b) $g_A^{(2)}(\tau)$ at $\lambda_A = 0.05$ and $\Gamma_{L,R} = 0.1\ \Gamma_{\mathrm{ph}}$ as a function of τ (solid line). The electric current autocorrelation function $g^{(2)}_{\mathrm{current}}(\tau)$ is also shown by a dotted line.

in the λ_A–$(\Gamma_{L,R}/\Gamma_{\mathrm{ph}})$ plane for $\Gamma_L = \Gamma_R \equiv \Gamma_{L,R}$ and $\lambda_S = 0$. At $\lambda_A = 0.05$ and $\Gamma_{L,R}/\Gamma_{\mathrm{ph}} = 0.1$, for example, $g_A^{(2)}(0) \ll 1$, representing a strong antibunching of phonons. This is because the phonon emission is regularized by the electron transport through the DQD. In Fig. 4(b), we plot the autocorrelation function of the electric current

$$g^{(2)}_{\mathrm{current}}(\tau) = \langle : n_R(0)n_R(\tau) : \rangle / \langle n_R\rangle^2, \quad (18)$$

where n_R is the electron number in dot R. It fulfills $g^{(2)}_{\mathrm{current}}(0) = 0$, indicating the antibunching of electron transport, since dot R is empty just after the electron tunnels out [26]. Remarkably, $g_A^{(2)}(\tau)$ almost coincides with $g^{(2)}_{\mathrm{current}}(\tau)$. Again at very strong couplings $\lambda_A \gtrsim 1$, neither phonon antibunching nor phonon lasing can be observed because of an effective phonon thermalization due to the Franck-Condon effect.

In our calculations, we have neglected the S-phonon coupling that, however, does not affect the dynamics of A-phonons as we have checked. We have also disregarded acoustic-phonon-assisted tunneling to excited levels in dot R because the energy of LA phonons at small wave numbers $|\boldsymbol{q}| \lesssim 1/\mathcal{R}$ is comparable to or lower than the spacing between the energy levels for $\mathcal{R} < 100$ nm, and the coupling to LA phonons is much weaker than that to LO phonons. Indeed, the LO-phonon-assisted transport was clearly observed for level spacings Δ tuned to $\hbar\omega_{\mathrm{ph}}$ and $2\hbar\omega_{\mathrm{ph}}$ in recent experiments [15].

Finally, we discuss possible experimental realizations to observe LO phonon lasing and antibunching in semiconductor-based DQDs. In GaAs, an LO phonon around the Γ point decays into an LO phonon and a TA phonon around the L point, which are not coupled to the DQD. These daughter phonons can be detected by

the transport through another DQD fabricated nearby [29, 30]. Alternatively, the modulation of the dielectric constant by the phonons could be observed by near-field spectroscopy [31]. With a decay rate $\Gamma_{\rm ph} \sim 0.1$ THz in GaAs [12], however, the lasing condition $\Gamma_{L,R} \gg \Gamma_{\rm ph}$ might be difficult to realize. Other materials with a longer lifetime of optical phonons, such as ZnO [32], may be preferable for observing the phonon lasing.

Our fundamental research of LO phonon statistics is also applicable to a freestanding semiconductor membrane as a phonon cavity [33, 34], in which a resonating mode plays a role of LO phonons. Our theory implies that a DQD could generate various quantum states of mechanical oscillators.

The authors acknowledge fruitful discussion with K. Ono, S. Amaha, Y. Kayanuma, K. Saito, C. Pöltl, T. Yokoyama, and A. Yamada. This work was partially supported by KAKENHI (No. 23104724 and No. 24-6574), the Institutional Program for Young Researcher Oversea Visits and the International Training Program from the Japan Society for the Promotion of Science, the Graduate School Doctoral Student Aid Program from Keio University, and the German DFG via SFB 910 and project BR 1528/8-1.

* rokuyama@rk.phys.keio.ac.jp

[1] O. Astafiev, K. Inomata, A. O. Niskanen, T. Yamamoto, Y. A. Pashkin, Y. Nakamura, and J. S. Tsai: Nature **449** (2007) 588.
[2] T. Brandes and N. Lambert: Phys. Rev. B **67** (2003) 125323.
[3] Ya. M. Blanter, O. Usmani, and Yu. V. Nazarov: Phys. Rev. Lett. **93** (2004) 136802 [Errata **94** (2005) 049904].
[4] D. A. Rodrigues, J. Imbers, and A. D. Armour: Phys. Rev. Lett. **98** (2007) 067204.
[5] H. Hübener and T. Brandes: Phys. Rev. Lett. **99** (2007) 247206.
[6] S. André, V. Brosco, A. Shnirman, and G. Schön: Phys. Rev. A **79** (2009) 053848.
[7] P. Gartner: Phys. Rev. A **84** (2011) 053804.
[8] J. McKeever, A. Boca, A. D. Boozer, J. R. Buck, and H. J. Kimble: Nature **425** (2003) 268.
[9] T. Fujisawa, T. H. Oosterkamp, W. G. van der Wiel, B. W. Broer, R. Aguado, S. Tarucha, and L. P. Kouwenhoven: Science **282** (1998) 932.
[10] T. Brandes and B. Kramer: Phys. Rev. Lett. **83** (1999) 3021.
[11] P. Roulleau, S. Baer, T. Choi, F. Molitor, J. Güttinger, T. Müller, S. Dröscher, K. Ensslin, and T. Ihn: Nat. Commun. **2** (2011) 239.
[12] F. Vallée: Phys. Rev. B **49** (1994) 2460.
[13] A similar situation was studied for the DQD coupled to the cavity photon by P.-Q. Jin, M. Marthaler, J. H. Cole, A. Shnirman, and G. Schön: arXiv:1205.0436.
[14] C. Gnodtke, G. Kießlich, E. Schöll, and A. Wacker: Phys. Rev. B **73** (2006) 115338.
[15] S. Amaha and K. Ono: private communications.
[16] J. Kabuss, A. Carmele, T. Brandes, and A. Knorr: Phys. Rev. Lett. **109** (2012) 054301.
[17] J. Koch and F. von Oppen: Phys. Rev. Lett. **94** (2005) 206804.
[18] S. Sapmaz, P. Jarillo-Herrero, Y. M. Blanter, C. Dekker, and H. S. J. van der Zant: Phys. Rev. Lett. **96** (2006) 026801.
[19] R. Leturcq, C. Stampfer, K. Inderbitzin, L. Durrer, C. Hierold, E. Mariani, M. G. Schultz, F. von Oppen, and K. Ensslin: Nat. Phys. **5** (2009) 327.
[20] The coupling to photons in a cavity corresponds to the weak coupling case, with dimensionless coupling constant $\lambda \sim 10^{-4}$ in ref. 8 and 10^{-2} in ref. 1, in Eq. (6).
[21] If a weak quadratic dispersion around the Γ point is taken into account, the collective phonon modes are scattered by the rate of $\gamma \sim \partial^2\omega_{\rm ph}/\partial q^2|_{q=0}/\mathcal{R}^2$, which is lower than the decay rate $\Gamma_{\rm ph}$ of LO phonons by two orders of magnitude in GaAs quantum dots with $\mathcal{R} = 10 \sim 100$ nm.
[22] T. Tasai and M. Eto: J. Phys. Soc. Jpn. **72** (2003) 1495.
[23] When the bias voltage is not sufficiently large, the current is suppressed by the Franck-Condon blockade. Here, we assume a large bias to avoid the blockade.
[24] S. Hameau, Y. Guldner, O. Verzelen, R. Ferreira, G. Bastard, J. Zeman, A. Lemaître, and J. M. Gérard: Phys. Rev. Lett. **83** (1999) 4152.
[25] M. O. Scully and M. S. Zubairy: *Quantum Optics* (Cambridge University Press, Cambridge, 1997).
[26] C. Emary, C. Pöltl, A. Carmele, J. Kabuss, A. Knorr, and T. Brandes: Phys. Rev. B **85** (2012) 165417.
[27] Supplemental Material [derivation of analytical expression for I, N_A, and $g_A^{(2)}(0)$ in Eqs. (15)–(17)] is provided online.
[28] N. Lambert and F. Nori: Phys. Rev. B **78** (2008) 214302.
[29] U. Gasser, S. Gustavsson, B. Küng, K. Ensslin, T. Ihn, D. C. Driscoll, and A. C. Gossard: Phys. Rev. B **79** (2009) 035303.
[30] D. Harbusch, D. Taubert, H. P. Tranitz, W. Wegscheider, and S. Ludwig: Phys. Rev. Lett. **104** (2010) 196801.
[31] J. Cunningham, M. Byrne, P. Upadya, M. Lachab, E. H. Linfield, and A. G. Davies: Appl. Phys. Lett. **92** (2008) 032903.
[32] C. Aku-Leh, J. Zhao, R. Merlin, J. Menéndez, and M. Cardona: Phys. Rev. B **71** (2005) 205211.
[33] E. M. Weig, R. H. Blick, T. Brandes, J. Kirschbaum, W. Wegscheider, M. Bichler, and J. P. Kotthaus: Phys. Rev. Lett. **92** (2004) 046804.
[34] J. Ogi, T. Ferrus, T. Kodera, Y. Tsuchiya, K. Uchida, D. A. Williams, S. Oda, and H. Mizuta: Jpn. J. Appl. Phys. **49** (2010) 045203.

Supplementary Material for "Optical Phonon Lasing in Semiconductor Double Quantum Dots"

Rin Okuyama[1], Mikio Eto[1], and Tobias Brandes[2]

[1] *Faculty of Science and Technology, Keio University, Yokohama 223-8522, Japan*
[2] *Institut für Theoretische Physik, Technische Universität Berlin, D-10623 Berlin, Germany*

In this supplemental material, we derive analytical expressions for the current I, number of phonons $\langle N_A\rangle$, and autocorrelation function of phonons $g_A^{(2)}(0)$ at the current subpeaks in Eqs. (15)–(17) in the main material. When $\Delta \simeq \nu\hbar\omega_{\rm ph}$, the energy eigenstates are given by the zero-electron states $|0,n\rangle = |0\rangle\otimes|n\rangle_A$, bonding and anti-bonding states between polarons $|\pm,n\rangle = \frac{1}{\sqrt{2}}\left(|L,n\rangle \pm |R,n+\nu\rangle\right)$, and polarons localized in dot R, $|R,n\rangle$ $(n=0,1,2,\ldots,\nu-1)$, in a good approximation for $V_C \ll \hbar\omega_{\rm ph}$, as mentioned in the main material. We have introduced polaron states $|L(R),n\rangle = |L(R)\rangle\otimes\mathcal{T}^{(\dagger)}|n\rangle_A$, with $\mathcal{T} = e^{-\lambda_A(a_A^\dagger - a_A)}$. The density matrix is given by

$$\rho = \sum_{n=0}^{\infty} P_{0,n}|0,n\rangle\langle 0,n| + \sum_{\sigma=\pm}\sum_{n=0}^{\infty} P_{\sigma,n}|\sigma,n\rangle\langle\sigma,n| + \sum_{n=0}^{\nu-1} P_{R,n}|R,n\rangle\langle R,n| \tag{19}$$

in the Born-Markov-Secular approximation. We define occupation number operators for zero-electron states, bonding and anti-bonding states between the polarons, and polarons localized in dot R as

$$n_0 = \sum_{n=0}^{\infty}|0,n\rangle\langle 0,n| = |0\rangle\langle 0|, \qquad n_{\rm mol} = \sum_{\sigma=\pm}\sum_{n=0}^{\infty}|\sigma,n\rangle\langle\sigma,n|, \qquad \tilde{n}_R = \sum_{n=0}^{\nu-1}|R,n\rangle\langle R,n|, \tag{20}$$

respectively. The relation of $n_0 + n_{\rm mol} + \tilde{n}_R = 1$ holds. The electron number in the DQD is given by $n_e = n_{\rm mol} + \tilde{n}_R = 1 - n_0$. The expectation values of the occupation numbers are

$$\langle n_0\rangle = \sum_{n=0}^{\infty} P_{0,n}, \qquad \langle n_{\rm mol}\rangle = \sum_{n=0}^{\infty} P_{{\rm mol},n}, \qquad \langle\tilde{n}_R\rangle = \sum_{n=0}^{\nu-1} P_{R,n}. \tag{21}$$

In the stationary state, the rate equations in Eqs. (12)–(14) in the main material yield

$$0 = -\Gamma_L P_{0,n} + \sum_{m=0}^{\infty}\frac{\Gamma_R}{2}|{}_A\langle n|\mathcal{T}^\dagger|m+\nu\rangle_A|^2 P_{{\rm mol},m} + \sum_{m=0}^{\nu-1}\Gamma_R|{}_A\langle n|\mathcal{T}^\dagger|m\rangle_A|^2 P_{R,m} + \Gamma_{\rm ph}\big[(n+1)P_{0,n+1} - nP_{0,n}\big], \tag{22}$$

$$0 = -\frac{\Gamma_R}{2}P_{{\rm mol},n} + \sum_{m=0}^{\infty}\Gamma_L|{}_A\langle n|\mathcal{T}|m\rangle_A|^2 P_{0,m} + \Gamma_{\rm ph}\left[\left(n+1+\frac{\nu}{2}\right)P_{{\rm mol},n+1} - \left(n+\frac{\nu}{2}\right)P_{{\rm mol},n}\right], \tag{23}$$

with $P_{{\rm mol},n} = P_{+,n} + P_{-,n}$ $(n=0,1,2,\ldots)$, and

$$0 = -\Gamma_R P_{R,n} + \Gamma_{\rm ph}\big[(n+1)P_{R,n+1} - nP_{R,n}\big], \tag{24}$$

with $P_{R,\nu} = P_{{\rm mol},0}/2$ $(n=0,1,2,\ldots,\nu-1)$.

CURRENT AND ELECTRON NUMBER

First, we express the current $I = e\Gamma_L\langle n_0\rangle$ in the stationary state. For the purpose, we sum up both sides of Eq. (22) over n. Using

$$\sum_{n=0}^{\infty}\left|{}_A\langle n|\mathcal{T}^\dagger|m\rangle_A\right|^2 = {}_A\langle m|\mathcal{T}\left(\sum_n|n\rangle_{AA}\langle n|\right)\mathcal{T}^\dagger|m\rangle_A = 1, \tag{25}$$

we obtain

$$0 = -\Gamma_L\langle n_0\rangle + \frac{\Gamma_R}{2}\langle n_{\rm mol}\rangle + \Gamma_R\langle\tilde{n}_R\rangle. \tag{26}$$

With $\langle n_0\rangle + \langle n_{\rm mol}\rangle + \langle \tilde{n}_R\rangle = 1$, we derive

$$\langle n_0\rangle = \frac{\alpha}{2+\alpha}(1+\langle\tilde{n}_R\rangle), \qquad \langle n_{\rm mol}\rangle = \frac{2}{2+\alpha}\left[1-(1+\alpha)\langle\tilde{n}_R\rangle\right], \tag{27}$$

with $\alpha = \Gamma_R/\Gamma_L$. These equations result in Eq. (15) in the main material:

$$I = e\Gamma_R\frac{1+\langle\tilde{n}_R\rangle}{2+\alpha}, \qquad \langle n_e\rangle = \frac{2-\alpha\langle\tilde{n}_R\rangle}{2+\alpha}. \tag{28}$$

The summation of Eq. (24) over n yields

$$\langle\tilde{n}_R\rangle = \frac{\nu\Gamma_{\rm ph}}{2\Gamma_R}P_{{\rm mol},0}. \tag{29}$$

PHONON NUMBER

Next, we derive the phonon number which is

$$\langle N_A\rangle = \sum_{n=0}^{\infty}P_{0,n}\langle 0,n|N_A|0,n\rangle + \sum_{\sigma=\pm}\sum_{n=0}^{\infty}P_{\sigma,n}\langle\sigma,n|N_A|\sigma,n\rangle + \sum_{n=0}^{\nu-1}P_{R,\nu}\langle R,n|N_A|R,n\rangle \tag{30}$$

$$= \sum_{n=0}^{\infty}nP_{0,n} + \sum_{n=0}^{\infty}\left(n+\frac{\nu}{2}+\lambda_A^2\right)P_{{\rm mol},n} + \sum_{n=0}^{\nu-1}(n+\lambda_A^2)P_{R,n} \tag{31}$$

$$\equiv \langle N_A n_0\rangle + \langle N_A n_{\rm mol}\rangle + \langle N_A\tilde{n}_R\rangle. \tag{32}$$

We have used

$$\mathcal{T}^\dagger N_A\mathcal{T} = (\mathcal{T}^\dagger a_A^\dagger\mathcal{T})(\mathcal{T}^\dagger a_A\mathcal{T}) = (a_A^\dagger-\lambda_A)(a_A-\lambda_A). \tag{33}$$

We multiply both sides of Eqs. (22)–(24) by n and sum up over n:

$$0 = -(\Gamma_L+\Gamma_{\rm ph})\langle N_A n_0\rangle + \frac{\Gamma_R}{2}\langle N_A n_{\rm mol}\rangle + \Gamma_R\langle N_A\tilde{n}_R\rangle + \frac{\nu\Gamma_R}{4}\langle n_{\rm mol}\rangle, \tag{34}$$

$$0 = \Gamma_L\langle N_A n_0\rangle - \left(\frac{\Gamma_R}{2}+\Gamma_{\rm ph}\right)\langle N_A n_{\rm mol}\rangle + \lambda_A^2\Gamma_L\langle n_0\rangle + \left(\frac{\nu+2\lambda_A^2}{4}\Gamma_R+\lambda_A^2\Gamma_{\rm ph}\right)\langle n_{\rm mol}\rangle + \Gamma_R\langle\tilde{n}_R\rangle, \tag{35}$$

$$0 = -(\Gamma_R+\Gamma_{\rm ph})\langle N_A\tilde{n}_R\rangle + \left[(\nu-1+\lambda_A^2)\Gamma_R+\lambda_A^2\Gamma_{\rm ph}\right]\langle\tilde{n}_R\rangle. \tag{36}$$

Here, we have used

$$\sum_{n=0}^{\infty}n\left|{}_A\langle n|\mathcal{T}^\dagger|m\rangle_A\right|^2 = {}_A\langle m|\mathcal{T}N_A\left(\sum_n|n\rangle_{AA}\langle n|\right)\mathcal{T}^\dagger|m\rangle_A = \sum_m{}_A\langle m|\mathcal{T}N_A\mathcal{T}^\dagger|m\rangle_A\ . \tag{37}$$

From Eqs. (34)–(36), we obtain Eq. (16) in the main material:

$$\langle N_A\rangle = (\nu+2\lambda_A^2)\frac{I}{e\Gamma_{\rm ph}} + \lambda_A^2\langle n_e\rangle. \tag{38}$$

PHONON AUTOCORRELATION FUNCTION

Finally, we derive the phonon autocorrelation function at zero time delay,

$$g_A^{(2)}(0) = \frac{\langle :N_A^2:\rangle}{\langle N_A\rangle^2} = \frac{\langle N_A^2\rangle - \langle N_A\rangle}{\langle N_A\rangle^2}, \tag{39}$$

where

$$\langle N_A^2\rangle = \sum_{n=0}^{\infty} P_{0,n}\langle 0,n|N_A^2|0,n\rangle + \sum_{\sigma=\pm}\sum_{n=0}^{\infty} P_{\sigma,n}\langle \sigma,n|N_A^2|\sigma,n\rangle + \sum_{n=0}^{\nu-1} P_{R,\nu}\langle R,n|N_A^2|R,n\rangle \tag{40}$$

$$= \sum_{n=0}^{\infty} n^2 P_{0,n} + \sum_{n=0}^{\infty}\left[n^2+\lambda_A^2(4n+1+\lambda_A^2)+\nu\left(n+\frac{\nu}{2}+2\lambda_A^2\right)\right]P_{\mathrm{mol},n} + \sum_{n=0}^{\nu-1}\left[n^2+\lambda_A^2(4n+1+\lambda_A^2)\right]P_{R,n} \tag{41}$$

$$\equiv \langle N_A^2 n_0\rangle + \langle N_A^2 n_{\mathrm{mol}}\rangle + \langle N_A^2\tilde{n}_R\rangle. \tag{42}$$

We multiply both sides of Eqs. (22)–(24) by n^2 and sum up over n. A similar technique to the last section leads to

$$0 = -(\Gamma_L+2\Gamma_{\mathrm{ph}})\langle N_A^2 n_0\rangle + \frac{\Gamma_R}{2}\langle N_A^2 n_{\mathrm{mol}}\rangle + \Gamma_R\langle N_A^2\tilde{n}_R\rangle + \Gamma_{\mathrm{ph}}\langle N_A n_0\rangle + \frac{\nu\Gamma_R}{2}\langle N_A n_{\mathrm{mol}}\rangle + \frac{\nu\lambda_A^2\Gamma_R}{2}\langle n_{\mathrm{mol}}\rangle, \tag{43}$$

$$0 = \Gamma_L\langle N_A^2 n_0\rangle - \left(\frac{\Gamma_R}{2}+2\Gamma_{\mathrm{ph}}\right)\langle N_A^2 n_{\mathrm{mol}}\rangle + 4\lambda_A^2\Gamma_L\langle N_A n_0\rangle + \left[\frac{\nu+4\lambda_A^2}{2}\Gamma_R + (\nu+1+8\lambda_A^2)\Gamma_{\mathrm{ph}}\right]\langle N_A n_{\mathrm{mol}}\rangle$$
$$+ \lambda_A^2(1+\lambda_A^2)\Gamma_L\langle n_0\rangle + \lambda_A^2\left[\frac{1-\nu-3\lambda_A^2}{2}\Gamma_R + (1-\nu-6\lambda_A^2)\Gamma_{\mathrm{ph}}\right]\langle n_{\mathrm{mol}}\rangle - \Gamma_R\langle\tilde{n}_R\rangle, \tag{44}$$

$$0 = -(\Gamma_R+2\Gamma_{\mathrm{ph}})\langle N_A^2\tilde{n}_R\rangle + \left[4\lambda_A^2\Gamma_R + (1+8\lambda_A^2)\Gamma_{\mathrm{ph}}\right]\langle N_A\tilde{n}_R\rangle$$
$$+ \left\{\left[(\nu-1)^2+\lambda_A^2(1-3\lambda_A^2)\right]\Gamma_R + \lambda_A^2(1-6\lambda_A^2)\Gamma_{\mathrm{ph}}\right\}\langle\tilde{n}_R\rangle. \tag{45}$$

From Eqs. (43)–(45), we find

$$\langle N_A^2\rangle - \langle N_A\rangle = 2\lambda_A^2\frac{\Gamma_L}{\Gamma_{\mathrm{ph}}}\langle N_A n_0\rangle + \left(\frac{\nu+2\lambda_A^2}{2}\frac{\Gamma_R}{\Gamma_{\mathrm{ph}}} + \frac{\nu+4\lambda_A^2}{2}\right)\langle N_A n_{\mathrm{mol}}\rangle + 2\lambda_A^2\left(\frac{\Gamma_R}{\Gamma_{\mathrm{ph}}}+2\right)\langle N_A\tilde{n}_R\rangle$$
$$- \frac{\nu+2\lambda_A^4}{2}\frac{\Gamma_L}{\Gamma_{\mathrm{ph}}}\langle n_0\rangle - \frac{\lambda_A^2(\nu+6\lambda_A^2)}{2}\langle n_{\mathrm{mol}}\rangle - \left[\frac{\nu(2-\nu)}{2}\frac{\Gamma_R}{\Gamma_{\mathrm{ph}}} + 3\lambda_A^2\right]\langle\tilde{n}_R\rangle. \tag{46}$$

Now we evaluate $g_A^{(2)}(0)$ in the case of $\Gamma_{L,R} \gg \Gamma_{\mathrm{ph}}$. In this case, $\langle\tilde{n}_R\rangle = \mathcal{O}(\Gamma_{\mathrm{ph}}/\Gamma_{L,R})$ from Eq. (29). Then

$$I = \frac{e\Gamma_R}{2+\alpha} + \mathcal{O}(\Gamma_{\mathrm{ph}}/\Gamma_{L,R}) \tag{47}$$

and

$$\langle N_A\rangle = \frac{\nu+2\lambda_A^2}{2+\alpha}\frac{\Gamma_R}{\Gamma_{\mathrm{ph}}} + \mathcal{O}(1). \tag{48}$$

Equations (34) and (36) yield

$$2\langle N_A n_0\rangle = \alpha\langle N_A n_{\mathrm{mol}}\rangle + \mathcal{O}(1), \qquad \langle N_A\tilde{n}_R\rangle = \mathcal{O}(\Gamma_{\mathrm{ph}}/\Gamma_{L,R}). \tag{49}$$

Using $\langle N_A\rangle = \langle N_A n_0\rangle + \langle N_A n_{\mathrm{mol}}\rangle + \langle N_A\tilde{n}_R\rangle$, we have

$$\langle N_A n_0\rangle = (\nu+2\lambda_A^2)\frac{\alpha}{(2+\alpha)^2}\frac{\Gamma_R}{\Gamma_{\mathrm{ph}}} + \mathcal{O}(1), \qquad \langle N_A n_{\mathrm{mol}}\rangle = (\nu+2\lambda_A^2)\frac{2}{(2+\alpha)^2}\frac{\Gamma_R}{\Gamma_{\mathrm{ph}}} + \mathcal{O}(1). \tag{50}$$

Using these relations, we obtain Eq. (17) in the main material:

$$g_A^{(2)}(0) = \frac{\nu+4\lambda_A^2}{\nu+2\lambda_A} + \mathcal{O}(\Gamma_{\mathrm{ph}}/\Gamma_{L,R}). \tag{51}$$